

- [.com/news-releases/glulam-connections-fire-test-report-now-available-300507431.html](http://www.fireresearch.com/news-releases/glulam-connections-fire-test-report-now-available-300507431.html).
- Seif, M., and T. McAllister. 2013. "Stability of wide flange structural steel columns at elevated temperatures." *J. Constr. Steel Res.* 84, 17–26.
- Seif, M., J. Main, J. Weigand, F. Sadek, L. Choe, C. Zhang, et al. 2016. *Temperature-dependent material modeling for structural steels: Formulation and application*. Gaithersburg, MD: NIST.
- SFPE (Society of Fire Protection Engineers). 2015. *Engineering standard on calculation methods to predict the thermal performance of structural and fire resistive assemblies*. SFPE S.02. Gaithersburg, MD: Society of Fire Protection Engineers.
- Wang, Y., I. Burgess, F. Wald, and M. Gillie. 2012. *Performance-based fire engineering of structures*. Boca Raton, FL: CRC Press.
- Wang, W., V. Kodur, X. Yang, and G. Li. 2014. "Experimental study on local buckling of axially compressed steel stub columns at elevated temperatures." *Thin-Walled Struct.* 82, 33–45.
- Zeng, D., K. Lo, K. Cheang, and J. Lai. 2013. "Remaining strengths and pitting resistance of AISI 316 after a fire attack: Implications for use as concrete rebars." *JMEPEG* 22, ASTM International (<https://slideheaven.com/remaining-strengths-and-pitting-resistance-of-aisi-316-after-a-fire-attack-impli.html>).
- Zhang, C., J. Gross, and T. McAllister. 2013. "Lateral torsional buckling of steel W-beams subjected to localized fires." *J. Constr. Steel Res.* 88, 330–338.
- Zhang, C., L. Choe, and Z. Zhang. 2014. "Behavior of axially loaded steel short columns subjected to a localized fire." *J. Constr. Steel Res.* 111, 103–111.

*This page intentionally left blank*

## CHAPTER 8

# MECHANICAL MATERIAL PROPERTIES

### 8.1 OVERVIEW

This chapter provides an overview of how the mechanical properties (e.g., elastic modulus, yield strength, and ultimate strength) of steel, concrete, masonry, and wood are affected by temperature. Some fundamental concepts about the effects of temperature on the mechanical properties of materials are covered, and references to the most widely accepted material models found in design codes and the research literature are provided. Available information is provided for completeness, and in some cases a range of experimental data from the literature is presented to show the degree of uncertainty in material properties at elevated temperatures. For many practical applications, the designer may default to one of the material models found in codes and standards (e.g., Eurocode, AISC, ACI); these models were designed to provide a suitable level of conservatism and have been thoroughly vetted within their intended scope of application.

It is recommended that the designer be judicious in the selection of material models for structural fire engineering design (SFED), keeping in mind the application that is under consideration:

- For forensic-level applications, which seek to match empirical observations, for instance, the designer is advised to use mechanical properties that match the stress–strain–temperature response of the actual materials used in construction as closely as possible. This may involve, for example, the use of *actual strength* rather than *nominal strength* in the stress–strain–temperature model.
- For design purposes, the designer is advised to use mechanical properties that provide some degree of conservatism. For instance, the

lower-bound estimates of strength and Young's modulus may be most appropriate. These may be determined from the contents of this chapter and/or from the research literature.

SFED analyses may be very sensitive to the material properties that are assumed. Therefore, it is good practice to perform a sensitivity analysis before selecting design values that are deemed critical to the SFED. Note that the response of materials to elevated temperatures is an active area of research, and in some cases (e.g., predicting spalling in concrete), there is a lack of industry consensus.

To model the temperature-dependent mechanical response of structural systems at elevated temperatures, the designer, at a minimum, should define a temperature-dependent stress–strain response for the material. This generally requires the specification of both (a) elastic response and (b) plastic behavior beyond the yield point as a function of temperature. Any material model referenced will require the values of both Young's modulus and Poisson's ratio to describe the linear, elastic behavior. Because the values of Poisson's ratio for different structural materials are relatively insensitive to changes in temperature, it is recommended that the designer use ambient values for SFED (CEN 2006, AISC 2016).

The nonlinear plastic behavior (i.e., beyond the yield point) can be described by providing yield stress as a function of strain at elevated temperatures. Predicting large deformations and fracture of elements using finite element programs requires information on the true stress–strain response of the material up to very large strains. A true stress–strain curve can be determined from an experimentally measured engineering stress–strain curve in a straightforward manner before the onset of necking for ductile materials (e.g., steel). However, after the onset of necking, determining the true stress–strain curve is more difficult because of the nonuniform deformation and complex state of stress and strain within the necked region of a tension test coupon.

Fire exposure can have residual effects on the stress–strain response of materials following cooling. The term *residual strength* herein refers to the strength of the material after it is heated by fire exposure to a specified temperature and then cooled to ambient temperature. SFED may involve analysis of the structural system following a fire event (e.g., analysis of structural elements that support building refuge areas). In these cases, the designer should define material properties based on the temperature that was reached during the fire event and, in some cases, the rate at which it was cooled (e.g., cooled by convection with air versus in water). Sections below provide residual material properties accordingly.

The designer should be aware that the data reported in the literature are often influenced by the mechanical testing regime used (e.g., steady-state versus transient-state test) and the assumptions made in defining the yield

strength of the material as a function of strain. Hence, the careless use of temperature-dependent stress–strain data could result in significant errors in an SFED. When modeling steel, for example, it is important for the designer to carefully consider how the yield strength is defined (e.g., using 0.2% offset strain or 2% total strain) and whether creep effects are implicitly included in the model or not. Similarly, the stress–strain–temperature response of concrete and masonry is highly dependent on the aggregate type, and the behavior of wood depends on its species, grade, and other contributing factors (e.g., direction of the loading). Accordingly, the designer should be familiar with the relevant factors that affect the response of materials at elevated temperatures to avoid significant modeling errors.

## 8.2 MECHANICAL PROPERTIES OF STEEL

### 8.2.1 Structural Steel

Important mechanical properties of structural steel such as yield stress, ultimate strength, proportional limit, and modulus of elasticity are all established using the fundamental stress–strain behavior at elevated temperatures. A variety of tests can be conducted to characterize the stress–strain behavior of steel at elevated temperatures, but the tension test is the most common.

**8.2.1.1 Stress–Strain–Temperature Response.** Under fire exposure, the stress–strain behavior of structural steel becomes time-dependent, especially for temperatures at or above 500°C (Morovat et al. 2012, Morovat 2014). For SFED applications, it is common practice to account for time effects indirectly through either loading rates or temperature rates. It is also possible to explicitly quantify time effects on the stress–strain behavior of structural steel when exposed to elevated temperatures.

**8.2.1.1.1 Rate- and Temperature-Dependent Response.** As mentioned previously, time effects on the stress–strain behavior of structural steel at elevated temperatures are often quantified indirectly as rate effects. To evaluate rate effects, two general types of material tests are performed. The first type of test is referred to as the steady-state temperature tension test, in which under constant temperature conditions, the time effects are implicitly considered through loading rates. The second type of test is referred to as the transient-state temperature tension test, in which under constant load conditions, time effects are implicitly considered through temperature rates. Choe et al. (2017) compared the mechanical properties of structural steels developed by these two different types of tension tests and evaluated the effects of stress–strain models used in the finite element models of structural steel columns at elevated temperatures.

**8.2.1.1.1 Steady-State Temperature Tension Test.** In steady-state temperature tension tests, the steel coupon temperature is first increased to the test temperature under no load (i.e., no restraint to thermal expansion). Static load is then monotonically increased while the temperature is held constant. The rate at which the static load is applied to the coupon is therefore the main factor affecting the mechanical behavior of steel obtained in a steady-state temperature tension test. For a specified temperature, steady-state temperature tension tests directly result in stress–strain curves corresponding to different loading rates. Note that most reported steel properties at elevated temperatures are based on steady-state temperature tension testing because of its simplicity and practicality (Outinen et al. 2001, Outinen and Mäkeläinen 2007, Lee et al. 2003, Lee et al. 2013). Luecke et al. (2011) provide a compilation of steady-state temperature tensions tests on structural steels.

Representative stress–strain curves determined from steady-state temperature tension tests of ASTM A992 structural steel specimens at various temperatures are shown in Figure 8-1. All the stress–strain curves shown in Figure 8-1 are from tests conducted at a constant crosshead displacement rate of 0.01 in./min. Figure 8-2 further plots the initial parts of the stress–strain curves in Figure 8-1 up to 0.5% strain. As shown in Figures 8-1 and 8-2, the fundamental shape of the stress–strain curve changes as temperature increases. Specifically, at 400°C and above, structural steel no longer exhibits a well-defined yield plateau, and it demonstrates significant nonlinearity at low levels of stress and strain. This

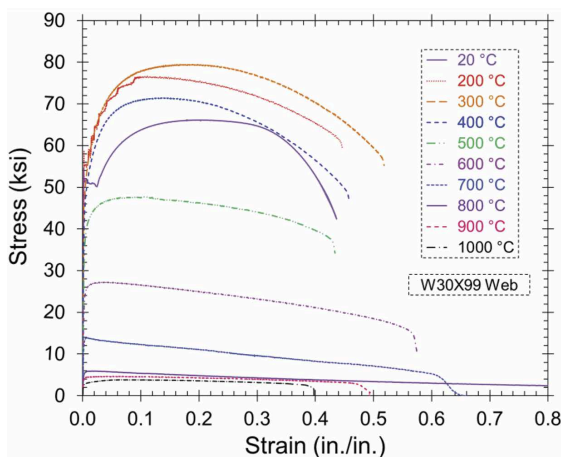


Figure 8-1. Engineering stress–strain curves of ASTM A992 steel at elevated temperatures obtained from steady-state temperature tension tests (entire curves). Source: Lee et al. (2013).

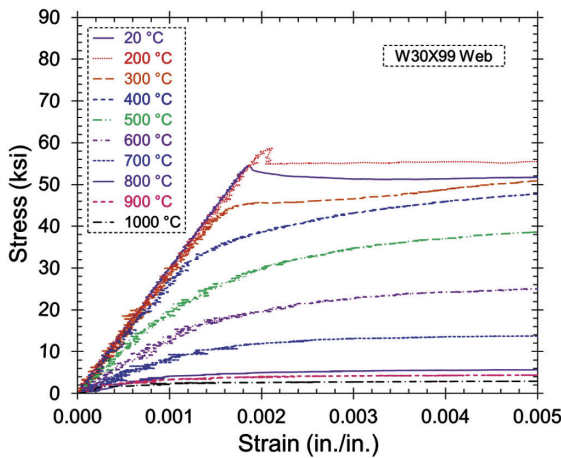


Figure 8-2. Engineering stress–strain curves of ASTM A992 steel at elevated temperatures obtained from steady-state temperature tension tests (initial portion of curves).

Source: Lee et al. (2013).

early nonlinearity may be particularly significant when considering the stability of a structure under fire exposure, wherein tangent stiffness is a critical material property. In addition, Figures 8-1 and 8-2 clearly show that the yield stress and modulus of elasticity decrease with the increase in temperature.

As stated, the loading rate is the major factor affecting the stress–strain curves of structural steel that are derived from a steady-state temperature tension test. For example, Figure 8-3 represents the effect of loading rate on the stress–strain curves of ASTM A992 structural steel determined from the steady-state temperature tension tests. The results are specifically shown for two constant crosshead displacement rates of 0.01 in./min and 0.10 in./min and two different temperatures of 600°C and 700°C. To illustrate the loading rate effects clearly, only the initial portions of the stress–strain curves up to 2% strain are plotted in Figure 8-3. The impact of the lower loading rate in reducing the yield and tensile strengths of ASTM A992 steel at elevated temperatures is clearly evident in Figure 8-3. More specifically, a displacement rate of 0.01 in./min results in yield and tensile strengths that are both 30% to 40% lower than those obtained at 0.10 in./min for the considered temperatures. Also, the lower loading rate results in higher nonlinearity in the *knee region* of the stress–strain curve of structural steel. This higher nonlinearity particularly affects both the buckling capacity and the thermally induced forces in steel columns subjected to elevated temperatures. Seif et al. (2016a) and Luecke et al. (2011) discuss a temperature-dependent stress–strain model that accounts for strain rate sensitivity. Overall, the

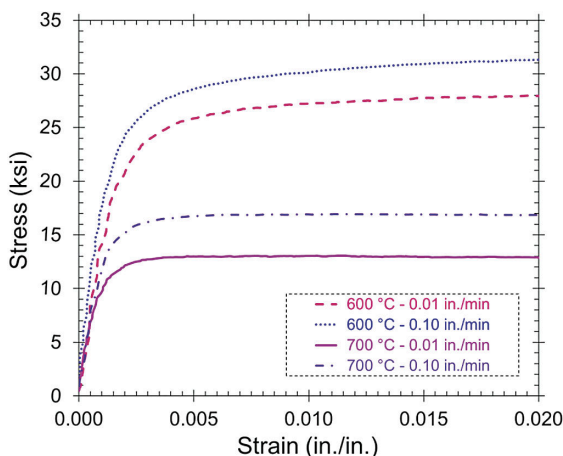


Figure 8-3. Loading rate effect on the engineering stress–strain curves of ASTM A992 steel at elevated temperatures obtained from steady-state temperature tension tests.

Source: [Lee et al. \(2013\)](#).

significant change in mechanical properties owing to variable loading rates is an indication of the time-dependent behavior of structural steel at elevated temperatures.

**8.2.1.1.1.2 Transient-State Temperature Tension Test.** In transient-state temperature tension tests, the steel coupon is first loaded to a target engineering stress level at ambient temperature. While holding the stress constant, the temperature is increased until fracture of the coupon occurs. Hence, the rate at which the temperature is increased is the main factor affecting the mechanical behavior of the steel. For a specified engineering stress, transient-state temperature tension tests result in strain–temperature curves corresponding to different heating rates. As a result, transient-state temperature tension tests do not directly result in stress–strain curves. A procedure that involves subtracting thermal strains from total measured strains and applying the cross-plotting technique is used to convert the strain–temperature curves into stress–strain curves at elevated temperatures (as shown in [Figure 8-4](#)). Details on the conversion can be found in the literature ([Kirby and Preston 1988](#); [Outinen et al. 2001](#); [Outinen and Mäkeläinen 2007](#); [Chen et al. 2006](#); [Schneider and Lange 2010](#)).

Representative strain–temperature curves for Grade 50B structural steel derived from transient-state temperature tension tests at various applied stresses are shown in [Figure 8-5](#). All strain–temperature curves presented in [Figure 8-4](#) are from tests conducted at a constant temperature rate of 10°C/min.

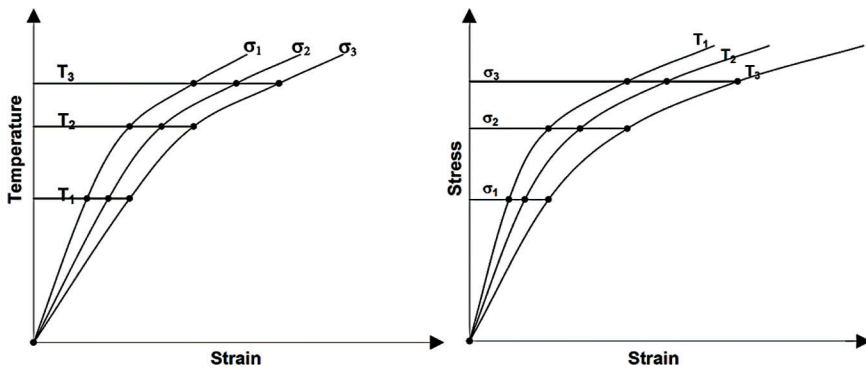


Figure 8-4. Constructing engineering stress–strain curves using strain–temperature curves obtained from transient-state temperature tension tests.

Source: [Outinen and Mäkeläinen \(2007\)](#).

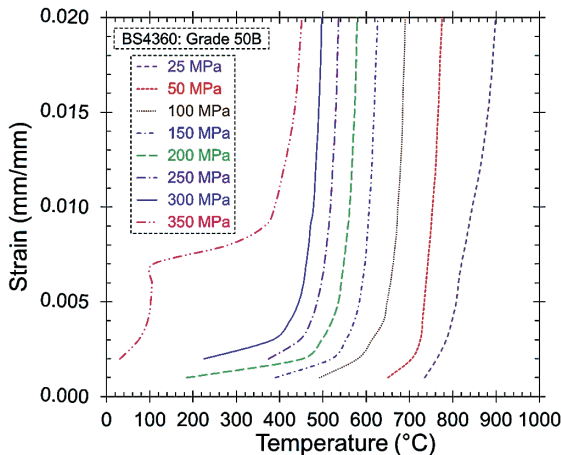


Figure 8-5. Engineering strain–temperature curves of Grade 50B steel obtained from transient-state temperature tension tests.

Source: [Kirby and Preston \(1988\)](#).

As stated, the heating rate can affect the strain–temperature curves of structural steel measured in a transient-state temperature tension test. For example, [Figure 8-6](#) illustrates the effect of heating rate on the strain–temperature curves of Grade 50B structural steel. Specifically, the results are shown for two constant temperature rates of 10°C/min and 20°C/min, and two different stress levels of 150 MPa and 350 MPa. For these tests, the impact of the higher heating rate in reducing the strains reached at a

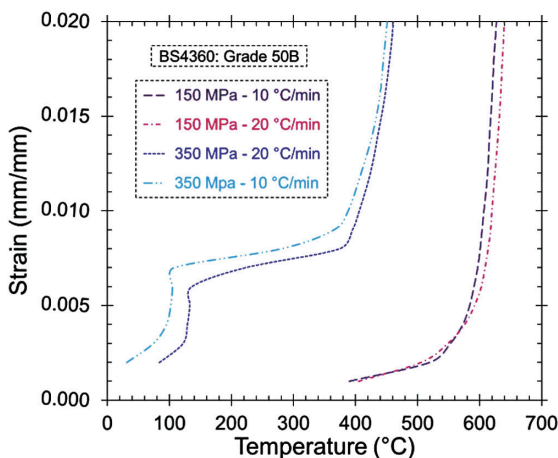


Figure 8-6. Temperature rate effect on engineering strain–temperature curves of Grade 50B steel obtained from transient-state temperature tension tests.

Source: *British Steel (1983), Kirby and Preston (1988).*

certain temperature is modest. However, time-dependent effects on the stress–strain behavior of steel should be accounted for when a transient-state temperature tension test is used.

**8.2.1.1.2 Time- and Temperature-Dependent Response.** In the previous section, material characterization tests were introduced to implicitly quantify the effect of time on the elevated-temperature behavior of steel for use in SFED. If required, the time effects on the stress–strain behavior of structural steel at elevated temperatures can be also directly evaluated. To explicitly account for time effects, two primary tension tests are conducted: the steady-state temperature creep test and the steady-state temperature relaxation test.

**8.2.1.1.2.1 Steady-State Temperature Creep Test.** The most common material characterization test to quantify the time-dependent behavior of structural steel at elevated temperatures is the steady-state temperature creep test in tension. This test is a force-controlled test in which the steel coupon temperature is first increased to the test temperature under no load. A load that produces a specific engineering stress is then quickly applied while the temperature is held constant. Both the stress and the temperature are subsequently held constant, and the strain is monitored for a specific period of time. At a specific temperature, steady-state temperature creep tests result in strain–time curves corresponding to different engineering stresses. A typical creep strain versus time curve is shown in [Figure 8-7 \(Morovat 2014\)](#). This curve is often divided into the three phases of primary,